PUBLISHED BY INSTITUTE OF PHYSICS PUBLISHING AND SISSA
RECEIVED: *March 5, 2007*
REVISED: *April 11, 2007*
ACCEPTED: *April 12, 2007*
PUBLISHED: *May 2, 2007*

An inexpensive spectroscopic beam monitor for hard X-ray synchrotron applications

A. Owens,[a*] S. Andersson,[a] R. den Hartog,[a] F. Quarati,[a] A. Webb[b] and E. Welter[b]

[a] *Science Payload and Advanced Concepts Office, ESA/ESTEC, Postbus 299, 2200AG Noordwijk, The Netherlands*
[b] *HASYLAB at DESY, Notkestrasse 85, D 22607 Hamburg, Germany*
E-mail: aowens@rssd.esa.int

ABSTRACT: We describe an inexpensive beam monitor for hard X-ray synchrotron applications which has good spectroscopic abilities and can operate without cooling. The device is centred on an inexpensive, commercial off-the-shelf, large area (1.2 × 1.2 mm^2) Si photodiode operated in single counting mode. Measurements carried out at the HASYLAB synchrotron research facility have shown that it is fully spectroscopic across the energy range 8 keV to 100 keV with a measured energy resolution of ~1.2 keV FWHM at room temperature. The measured resolutions were found to be the same under pencil-beam and full-area illumination, indicating uniform crystallinity and stoichiometry of the bulk. The low cost, simplicity and performance of the detector make it suitable for a wider range of applications, e.g., in undergraduate laboratory experiments.

KEYWORDS: Beam-line instrumentation (beam position and profile monitors; beam-intensity monitors; bunch length monitors); Instrumentation for synchrotron radiation accelerators; X-ray detectors.

* Corresponding author.

2007 JINST 2 P05002

Contents

2007 JINST 2 P05002

1. Introduction

The Science Payload and Advanced Concepts Office of ESA has worked for a number of years to produce semiconductor detection planes in conjunction with light-weight X-ray optics. The ultimate goal of this program is to produce Fano limited, mega-pixel soft and hard X-ray imagers with arc-second angular resolution for future planetary and astrophysics space missions. The detector research program has centered on compound semiconductors, including, GaAs, InP, $Cd_{(1-x)}Zn_xTe$, HgI_2 and TlBr and results have been reported elsewhere [1]. Much of the work is carried out at Synchrotron Research facilities. Key to the measurement program is the use of several reference detectors. These are used for a variety of purposes as well as general beam monitoring. For example, locating and positioning the beam, checking the spectral purity of the beam and adjusting the beamline control accordingly, measuring the efficiency of test detectors and determining depletion depths. At present, we use several Amptek detectors [2], the choice of which depends on the particular measurement. These detectors invariably get damaged during the rigors of many experimental campaigns - in particular the beam monitor which tends to get more use than the specialized detectors. Replacement of this detector is expensive and so what is ideally required is a general purpose beam monitor that is inexpensive, of size ~1 mm^2, low bias, spectroscopic ($E/\Delta E>10$), simple operation and radiation hard. In a survey of possible sensors, it became apparent that some fast photo-detectors may have the required detection area and low enough leakage currents to allow spectroscopic measurements. In fact, a literature search revealed that Si photodiodes have been used previously to record broad-band soft X-ray emissions from plasma focusing devices [3]. A number of commercial off-the-shelf photodiodes were procured and tested. The photodiode which showed the most promise was a BXP65 device [4] which is described in the specification sheet as a fast optical sensor for fibreoptic communication applications. The typical “one-off” price is < 10 euros.

2. The detector

The photodiode is a c-Si:H surface-diffused junction with a thick intrinsic region between p and n. It is packaged in an open TO18 metal housing which is covered with a thin flat glass window (see figure 1, left). The glass serves two functions. It hermetically seals the can and allows the

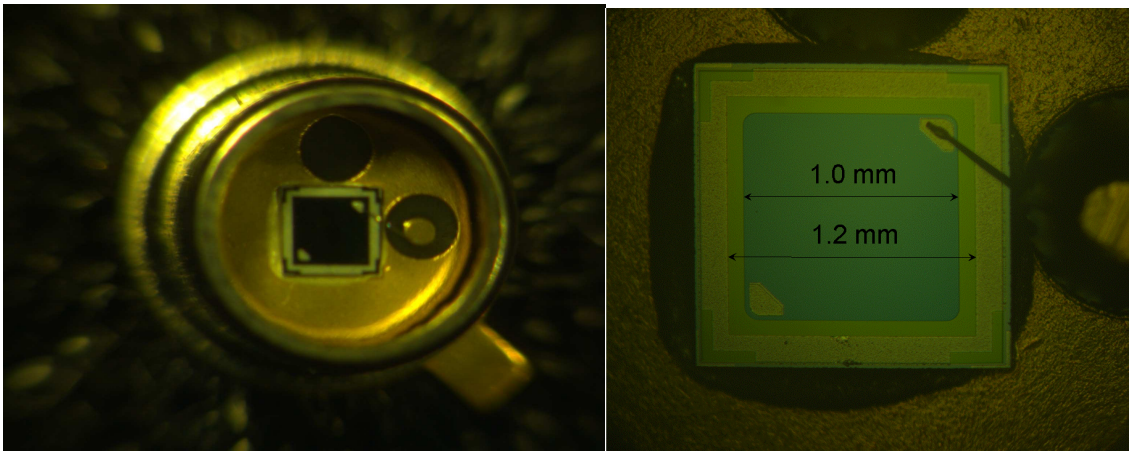

Figure 1. Left: photograph of the detector. Right Nomarski photomicrograph of the chip. The bond wire is clearly visible in the upper right hand corner. The inner dark green square has dimensions 1.0×1.0 mm^2. The dimensions up to the guard ring are 1.2×1.2 mm^2.

transmission of light to the phoosensitive surface. A Nomarski photomicrograph of this surface is shown in figure 1 (right). The chip appears to be attached to the die by silver epoxy. Thus, the cathode is electrically connected to the case. A bond wire is clearly visible in the upper right hand corner which terminates on the anode pin out. The inner dark green area is presumably the optical surface - since it has dimensions 1×1 mm^2 [4]. Later X-ray microbeam mapping revealed that the active X-ray area actually extends to the guard ring and is 1.2×1.2 mm^2.

The manufacturers specifications state that reverse biases of up to 50V can be applied. However, above 20V the noise was observed to increase considerably. For the experiments described here, the applied bias was set at 10V. At this bias, the leakage current is ~1nA, which should be low enough to ensure that the device is spectroscopic at soft X-ray wavelengths. The capacitance of the device at this bias was ~3 pF and is ideally matched to the input of the preamplifier, which is a resistive feedback charge sensitive type. Lastly, at the nominal operating bias, the depletion depth will be of the order of 10 µm which means that the device will be inefficient at hard X-ray wavelengths. For example, at 10 keV the efficiency is 8%. This not seen as a problem for synchrotron applications, since the beam intensity is usually much too high for most beam monitors to operate in single photon counting mode without considerable detuning of the monochromator. Certainly, above say 30 keV the device can function well as both a spectrometer and a beam intensity monitor with little adjustment of the beam.

The entire assembly is hermetically sealed in a test package. X-rays are viewed through a thin (25 µm), vacuum tight beryllium window. The rest of the analog chain consists of an Ortec 671 spectroscopy amplifier whose output is digitized by an Amptek MCA8000A 12-bit ADC and stored on a PC.

In figure 2, we show measured energy-loss spectra from full-area exposures to ^{109}Cd (a) and ^{241}Am (b) radioactive sources. The electronic shaping time was 3 µs. The FWHM energy resolutions of the principal lines at 22.1 keV and 59.5 keV are 1.15 keV FWHM. From figure 2, we see that the energy resolution is such that the ^{109}Cd Kβ line and the ^{241}Am L-edge sequence of neptunium lines are resolved. The corresponding system noise, as determined by a precision electronic pulser, was 2 keV FWHM. The noise floor, which we define to be the lowest energy for which the low energy noise attains an amplitude of 0.5 of the photopeak occurs at ~3 keV. No response at 6 keV could be detected from an ^{55}Fe source. Later removal of the cover glass

2007 JINST 2 P05002

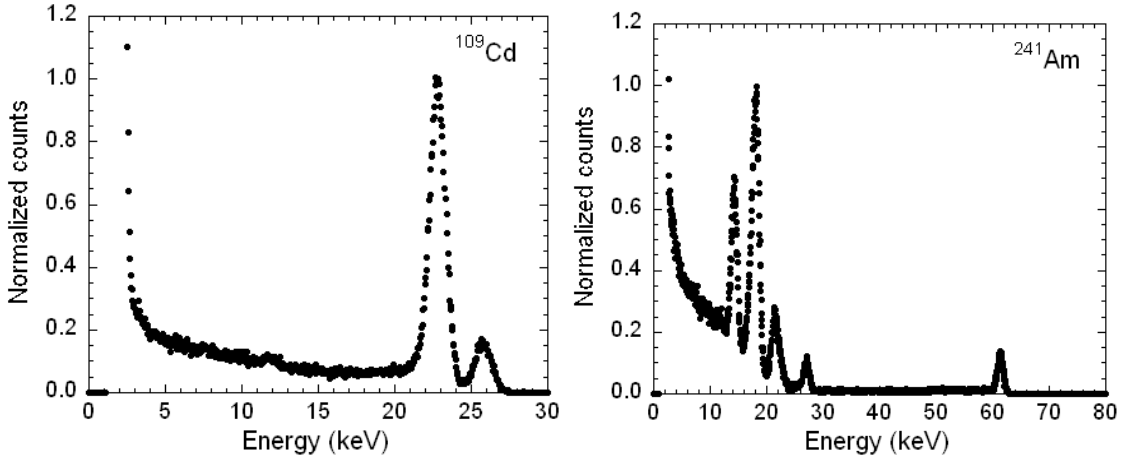

Figure 2. The measured response of a 1.44 mm^2 Si photo-detector to (a) ^{109}Cd and (b) ^{241}Am radioactive sources under full-area illumination.

showed it to be 1 mm thick, which will attenuate 5.9 keV photons by a factor of ~10^8. ^{55}Fe measurements without the cover glass gave a FWHM resolution of 1.2 keV.

3. Synchrotron X-ray measurements

X-ray characterization was carried out at the X-1 beamline at the Hamburger Synchrotronstrahlungslabor (HASYLAB) radiation facility in Hamburg, Germany [5]. This beamline utilizes a double Si crystal monochromator to produce highly monochromatic X-ray beams across the energy range 10 keV to 100 keV. To achieve such a large energy range, a [511] reflection was used, yielding an intrinsic energy resolution of ~1 eV at 10 keV rising to 20 eV at 100 keV. The beam spot size was set by a pair of precision stepper-driven slits, positioned immediately in front of the detector. The beamline employs a MOSTAB (MOnochromator STABilizer) servo loop system to ensure constant beam intensity at the detector. The detector was mounted on an X-Y table capable of positioning it to a precision of < 1 μm in each axis with respect to the beam. For the measurements described here the beam was normally incident at the center of the forward face of the detector. For the majority of the measurements, a slit size of 20×20 μm^2 was used. All measurements were carried out at room temperature. For completeness, additional full-area illumination measurements were also carried out using ^{109}Cd and ^{241}Am radioactive sources.

In figure 3, we show the variations of the FWHM energy resolution with amplifier shaping time. The measurements were carried out at an incident energy of 13.3 keV. The solid line shows the expected noise curve and the dashed and dotted lines its constituent components. As expected, we see that parallel noise dominates at large shaping times and varies as ~$\tau^{0.5}$, where τ is the shaping time. Its magnitude is determined primarily by the leakage current. At small shaping times, serial noise, which varies as ~$l/\tau^{0.5}$, is dominant. Flicker noise (l/f noise) appears to be negligible. Based on this graph a shaping time of 3 μs was used for the rest of the measurements. The right hand axis of figure 3 shows the noise floor which achieves a lowest value of ~1.6 keV. This would represent the lowest energy the detector could operate at, if the glass lens was removed.

2007 JINST 2 P05002

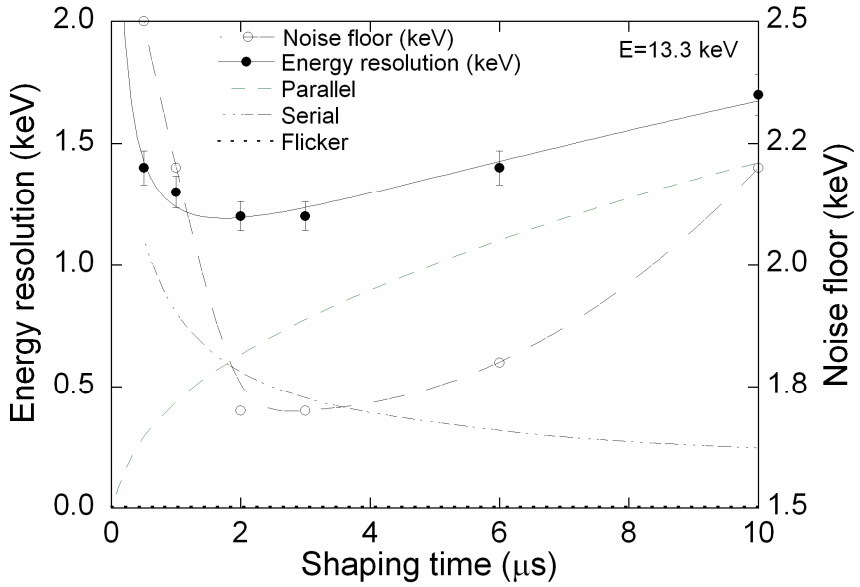

Figure 3. The variation of the FWHM energy resolution at an incident energy of 13.3 keV with amplifier shaping time constant. For completeness, we also show the individual components of noise, e.g., serial, parallel and flicker-noise.

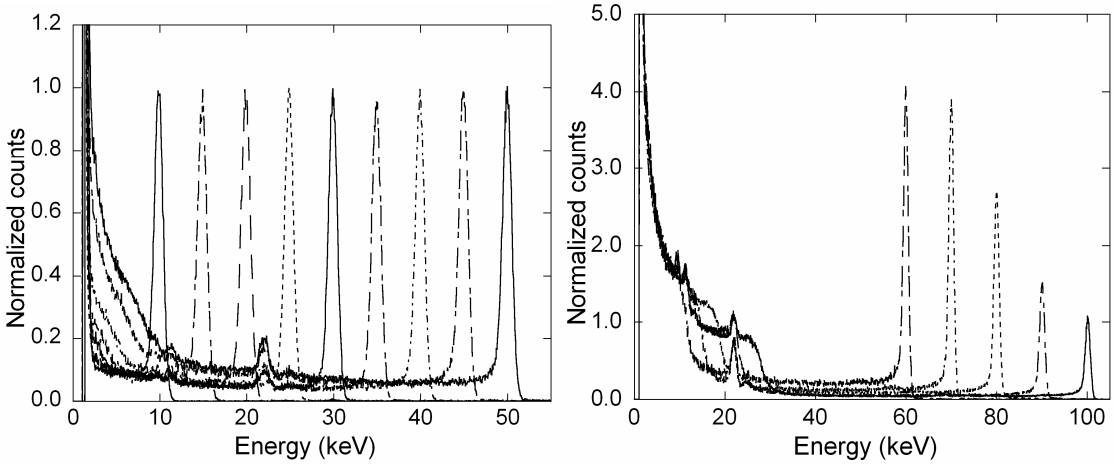

Figure 4. Composite of energy loss spectra measured at the center of the detector. Left: the low energy response and Right: the high energy response. At the higher energies, Compton edges are clearly visible.

3.1 Energy response

Figure 4 shows a composite of the detectors response to a series of highly collimated monochromatic spectral lines taken at HASYLAB. The beams were incident at the center of the detector. The detector energy response function was found to be linear over the energy range 8 keV to 100 keV with an average rms non-linearity of 0.3%, consistent with statistics. Below ~60 keV, the recorded events are confined almost entirely to the photopeaks which are very nearly Gaussian and the level of continuum is low, being ~5% of the photopeak amplitude. Above ~60 keV, Compton edges become apparent at lower energies. The noise floor occurs at ~2 keV. Fluorescent K-shell lines from Ag and L-shell lines from Au are apparent in the spectra. These are illustrated in figure 5 in which we show the spectrum accumulated at an

2007 JINST 2 P05002

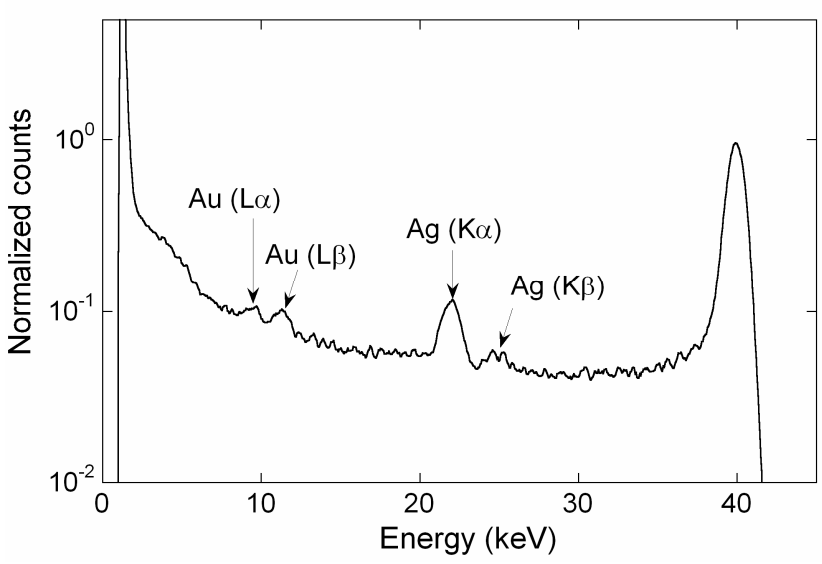

Figure 5. Detailed spectrum at 40 keV. Note fluorescent Ag K lines at 22.1 keV and 25 keV and Au L lines near 10 keV.

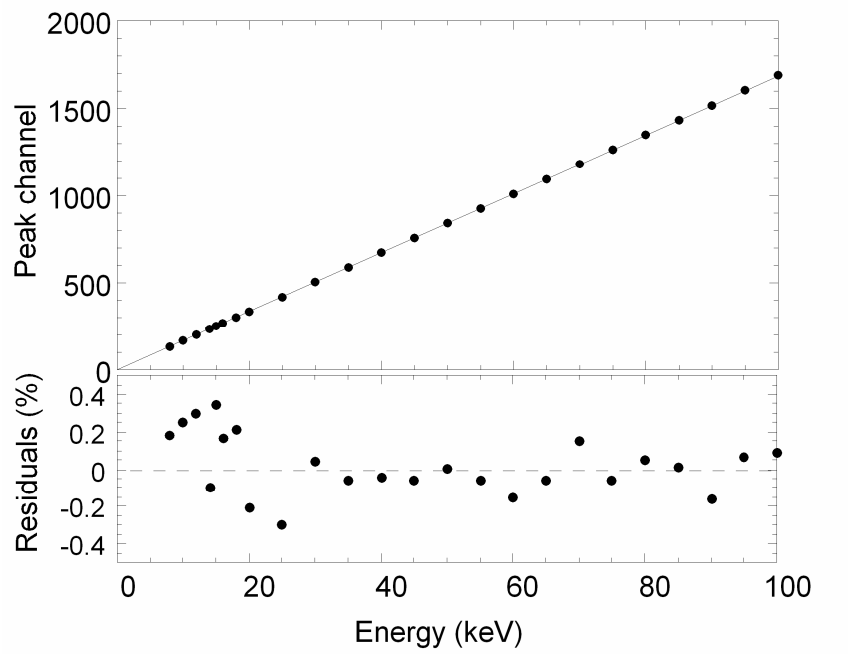

Figure 6. The linearity of the detector measured over the energy range 8 keV to 100 keV. The solid lines show best-fit linear regression. The lower panels shows the residuals, i.e. (measured energy-energy)/ energy × 100%.

incident energy of 40 keV. In fact, weak Au Kα1 at 68.8 keV and Kα2 at 67.0 keV are apparent and nearly resolved in the 90 keV and 100 keV spectra. The Au lines presumably arise from the contacts and the Ag lines from the epoxy used to secure the chip to the die.

The detected charge response to X-ray absorption was found to be remarkably linear with photon energy. The regression coefficients for a best-fit linear function to the peak channel number versus incident X-ray energy is in excess of 99.99% across the entire energy range. In figure 6, we show the detector linearity curve. The non-linearity was determined from the

2007 JINST 2 P05002

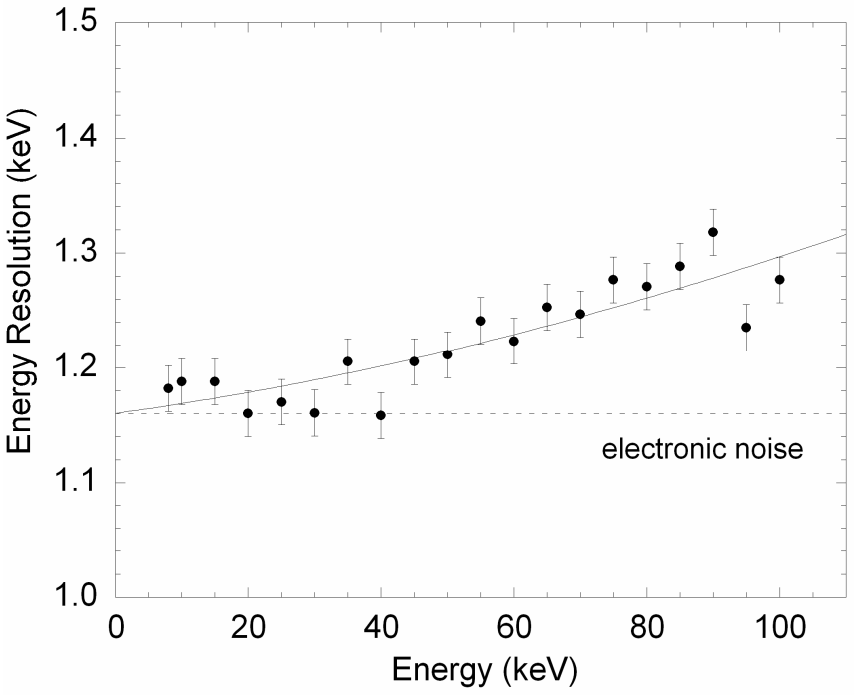

Figure 7. Measured energy resolution across the energy range 8 keV to 100 keV. The solid line is a best fit of the expected resolution function to the data (see text).

residuals of a best-fit linear regression to the measured line centre energies. The rms non-linearity is ≤ 0.3%, consistent with the statistical error in the fit. The lower panel of figure 6 shows the individual residuals of the fit, i.e., (measured energy - energy)/ energy × 100% from which we can see there are no systematic trends with energy.

The energy resolutions determined from figure 7, range from 1.16 keV FWHM at 8 keV to 1.3 keV FWHM at 100 keV. The solid line in figure 7 shows the best-fit expected resolutions, assuming them to be a convolution of three noise sources (Fano noise, noise due to inefficient charge collection and electronic noise). Assuming all three are independent normally distributed variables, the resolution function has the semi-empirical form,

$$\Delta E = 2.355\sqrt{F\varepsilon E + a_1 E^2 + \left(\Delta E_e / 2.355\right)^2} \qquad (1)$$

where F is the Fano factor, ε is the energy to create an electron-hole pair, a_1 is an empirical constant determined by best-fitting, ΔE_e is the F of the electronic noise and E is the incident energy. The electronic noise component, ΔE_e was directly measured using a precision electronic pulser to be 1.16 keV FWHM. From the fit, we find that electronic noise dominates the resolution function, being at least a factor of 3 greater than the other two components.

3.2 Spatial response

The spatial response of the detector was evaluated at HASYLAB using a 12 keV collimated beam of size 40×40 μm^2, normally incident on the detectors forward detection area. The beam was then raster scanned across this area with a spatial resolution of 20 μm. Spectra were accumulated at each position for a fixed time interval and the total count rate above a 2 keV threshold, the peak centroid position and the FWHM energy resolution determined by best-fitting. The results are shown in figure 8, for each of the recorded parameters. These data

2007 JINST 2 P05002

represent the output of 4290 individual spectral accumulations across the detector. Note, the energy resolution is displayed in terms of its resolving power (i.e., E/ΔE) to ensure numerical stability across the detector boundaries (i.e., that the function goes to zero outside the active area). From the individual distributions, we see that the detectors response is very uniform. In fact, the non-uniformity is typically no worse than a few percent across the surface and is consistent with a flat response – i.e., the variations seen in each distribution being consistent with the expected statistical variation, i.e, a) = 2%, b) =0.14% and c) = ~10% (limited primarily by the fitting algorithm). The average FWHM energy resolution recorded at each data point was 1.2 keV. For comparison, the energy resolution of the sum of all 4290 spectral accumulations was also 1.2 keV. Surprisingly, the detectors actual sensitive area was found to be 1.2×1.2 mm^2. Inspection of the Normarski photomicrograph (see figure 1, right) showed that these are the dimensions up to the guard ring. The inner dark green area in figure 1 (right) has dimensions 1.0×1.0 mm^2 and is presumably an etch through the outer passivation layer to uncover the optically sensitive surface.

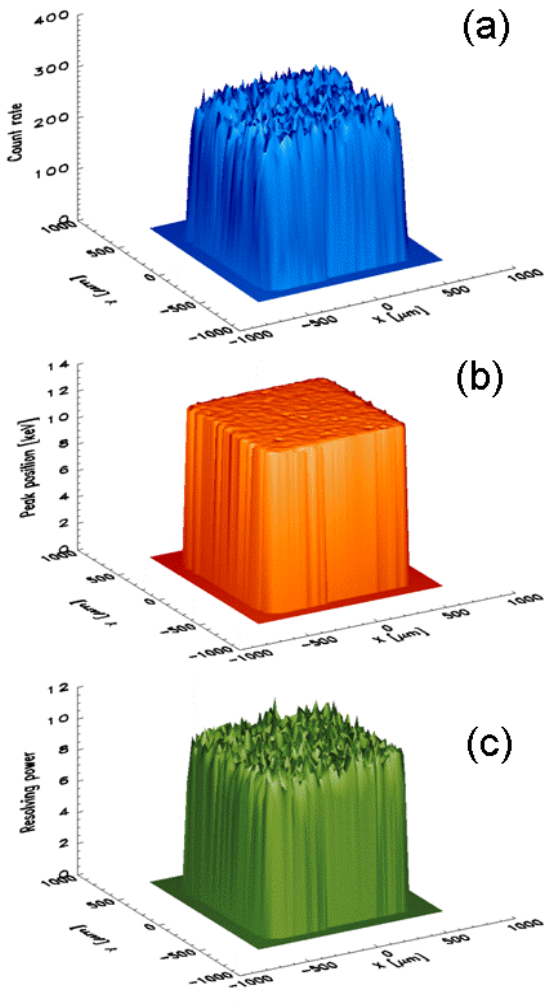

Figure 8. The spatial response of the detector measured at HASYLAB using a 40×40 μm^2, 12 keV X-ray beam. (a) shows the variation in count rate profile, (b) the fitted centroid of the photopeak, and (c) the resolving power, i.e., E/ΔE. These distributions were derived from spectra accumulated at 4290 positions across the detector.

4. Discussion and conclusions

The present work has shown that it is possible to construct a very inexpensive beam monitor using a commercial off-the-shelf sensor. In fact, the performance of the device is good enough to consider its use in general spectroscopic applications such as XRF and PIXE studies of heavy elements. Removal of the glass lens will improve the low energy response so general XRF applications can be considered, as well as beam monitoring on low energy beamlines. However, for detector operation in air (where there is effectively an 8 keV threshold), retaining the glass is beneficial, since it acts as a low energy filter, reducing noise. Needless to say, the major component of system noise (the leakage current) could be reduced by cooling, substantially improving energy resolution. Given the cost of the sensitive element (< 10 euros), the device is ideal for high risk measurements. The construction of large area arrays of diodes may also be attractive for some applications.

This work was supported by the IHP-Contract II-04-016 EC of the European Commission.

References

[1] A. Owens et al., *Development of compound semi-conductor detectors for X- and gamma-ray spectroscopy, Proc. of the SPIE* **4784** (2003) 244.

[2] http://www.amptek.com/

[3] J.Y. Tan, S. Kanesan, A.C. Petran, R.S. Rawat and P. Lee, *Investigations of X-rays ~5-30 keV from a 3kJ dense plasma focus using silicon detectors,* 30th EPS Conference on Contr. Fusion and Plasma Phys., ECA **27A** (2003) 2.62.

[4] http://www.msc-ge.com/download/Centronic/fotodet/EOSeriesBPX65.pdf

[5] http://www-hasylab.desy.de/

2007 JINST 2 P05002